

Anne Vuorema · Philip John ·  
A. Toby A. Jenkins · Frank Marken

## A rotating disc voltammetry study of the 1,8-dihydroxyanthraquinone mediated reduction of colloidal indigo

Received: 18 January 2006 / Revised: 14 February 2006 / Accepted: 16 March 2006 / Published online: 10 May 2006  
© Springer-Verlag 2006

**Abstract** Colloidal indigo is reduced to an aqueous solution of leuco-indigo in a mediated two-electron process converting the water-insoluble dye into the water-soluble leuco form. The colloidal dye does not interact directly with the electrode surface, and to employ an electrochemical process for this reduction, the redox mediator 1,8-dihydroxyanthraquinone (1,8-DHAQ) is used to transfer electrons from the electrode to the dye. The mediated reduction process is investigated at a (500-kHz ultrasound-assisted) rotating disc electrode, and the quantitative analysis of voltammetric data is attempted employing the Digisim numerical simulation software package. At the most effective temperature, 353 K, the diffusion coefficient for 1,8-DHAQ is  $(0.84 \pm 0.08) \times 10^{-9} \text{ m}^2 \text{ s}^{-1}$ , and it is shown that an apparently kinetically controlled reaction between the reduced form of the mediator and the colloidal indigo occurs within the diffusion layer at the electrode surface. The apparent bimolecular rate constant  $k_{\text{app}} = 3 \text{ mol m}^{-3} \text{ s}^{-1}$  for the rate law  $\frac{d[\text{leuco-indigo}]}{dt} = k_{\text{app}} \times [\text{mediator}] \times [\text{indigo}]$  is determined and attributed to a mediator diffusion controlled dissolution of the colloid particles. The average

particle size and the number of molecules per particles are estimated from the apparent bimolecular rate constant and confirmed by scanning electron microscopy.

**Keywords** Indigo · Colloid · Mediator · Reduction · Dye · Rotating disc · Voltammetry · Ultrasound · Sonoelectrochemistry · Digisim

### Introduction

The reduction of indigo to leuco-indigo represents an important type of industrial process which is operated worldwide on a considerable scale [1]. To improve this type of process by eliminating or minimizing the production of inorganic waste from chemical reducing agents, the biological [2] and the electrochemical reduction of indigo have been proposed [3]. In recent years several novel electrochemical processes have been developed. The direct electrochemical reduction of indigo is hindered by a very high activation barrier due to the insoluble particulate (colloidal) nature of the dye in aqueous environments [4]. Only strong adsorption, for example, at mercury electrodes, has been reported to overcome this problem [5]. The extremely low solubility of indigo is due to extensive hydrogen binding within the structure [6]. Only when firmly immobilized onto a graphite electrode surface have direct electrochemical processes for the solid indigo been observed [7]. In a study exploring the solid-state electrochemical properties of indigo, the effects of pH, electrolyte, and convection have been investigated [7]. Mediator-based reactions with the Fe(III) triethanolamine (TEA) complex [8] and with  $\text{Fe}^{3+}$ -D-gluconate or  $\text{Ca}^{2+}$ - $\text{Fe}^{3+}$ -D-gluconate complexes [9] have been proposed. Anthraquinone derivatives have been investigated as mediators in both the bacterial [10] and the electrochemical [11] reduction of indigo, although there is essentially no quantitative kinetic and mechanistic information available. The direct reduction of indigo in fixed and fluidized beds [12], nickel [13], or zinc contacts represent alternative mediator-free approaches. Pre-reduced indigo was introduced where the

Dedicated to Professor Dr. Alan M. Bond on the occasion of his 60th birthday

A. Vuorema · P. John  
School of Biological Sciences, The University of Reading,  
P.O. Box 221, Reading RG6 6AS, UK

A. Toby A. Jenkins · F. Marken (✉)  
Department of Chemistry, University of Bath,  
Bath BA2 7AY, UK  
e-mail: f.marken@bath.ac.uk

A. Vuorema  
Plant Production Research, Crops and Biotechnology,  
MTT Agrifood Research Finland,  
31600 Jokioinen, Finland

leuco-indigo is assisting reduction via a catalytic hydrogenation process. The commercial leuco-indigo product is sold as a 40 % solution to the dye houses [14].

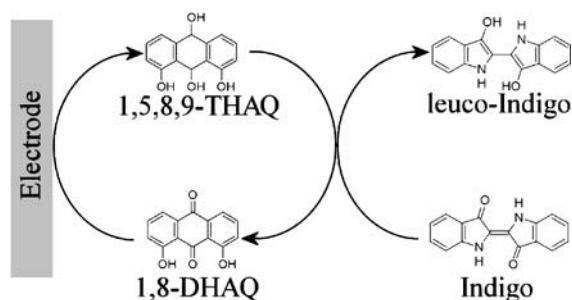
In spite of the development of several types of processes, very little is known about the mechanism and kinetics associated with the reduction of colloidal indigo. Therefore, this study aims at investigating and quantifying the mediator-based electrochemical reduction of colloidal indigo.

In this report 1,8-dihydroxyanthraquinone (1,8-DHAQ; see Scheme 1) is introduced as an effective redox mediator. The reversible potential for the mediator reduction [in 0.1 M phosphate buffer (pH 12, 353 K)]  $E^{\circ} = -0.78$  V vs saturated calomel electrode (SCE) is virtually identical to the reversible potential for the direct reduction of solid indigo ( $E^{\circ} = -0.78$  V vs SCE) and therefore highly effective. It is shown that in spite of the low overpotential, a very fast (essentially diffusion-controlled) reduction and solubilisation of indigo occurs. The physicochemical properties of this mediator system have been studied and (ultrasound-assisted) rotating disc electrode experiments performed to quantify the interaction between mediator and dye particles. Elevated temperatures are shown to be beneficial, and 500 kHz ultrasound is demonstrated to provide stable conditions for colloidal electrochemistry without significantly affecting the rate of the electrochemical reduction process. Data analysis is demonstrated based on a commercially available numerical simulation software package (Digisim3, Cyclic voltammetric simulator for Windows, version 3.03, BASi, USA [15]), and a quantitative mechanistic model consistent with diffusion-controlled interfacial kinetics is proposed.

## Experimental

### Reagents

Chemical reagents such as indigo (Fluka), phosphoric acid, NaOH, and 1,8-DHAQ (Sigma-Aldrich) were obtained commercially and used without further purification. Demineralised water was taken from an Elga purification system with at least 15 M  $\Omega$  cm resistivity. Argon gas was employed for de-aeration and obtained from BOC.



**Scheme 1** Diagrammatic representation of the 1,8-dihydroxyanthraquinone mediated reduction of indigo to leuco-indigo

### Instrumentation

For voltammetric studies a micro-Autolab II potentiostat system (EcoChemie, Netherlands) was employed with a Pt mesh counter electrode and a SCE reference electrode (Radiometer, Copenhagen). A 7-mm-diameter rotating gold disk electrode was used as the working electrode in experiments with colloidal solutions. A 4.9-mm-diameter basal plane pyrolytic graphite electrode was employed for solid-state voltammetry experiments [16, 17]. The home-built electrochemical cell was thermostated (with a Haake B3 circulator) and equipped with an ultrasound transducer (Undatim, 100 W, 500 kHz) to minimize sedimentation effects (see Fig. 1). Control experiments in the presence and in the absence of 500 kHz ultrasound were recorded to avoid direct effects of ultrasound on the electrochemical process. Only at a rate of electrode rotation lower than 1 Hz were additional ultrasound mass transport effects observed. Experiments were conducted under constant de-aeration with high-purity argon. Indigo dispersions were prepared by sonication (24 kHz, Hielscher UP200s glass horn probe) for 5 min in aqueous buffer and injection into the bulk buffer solution. Although stable for several hours, these dispersions may not be regarded as stable colloidal solutions due to the slow precipitation of indigo. To avoid precipitation and non-homogeneous conditions, 500 kHz ultrasound was introduced. Scanning electron microscopy (SEM) images were obtained with a JEOL JSM6310 system. Unless stated otherwise, the temperature was controlled at  $80 \pm 2$  °C (353 K).

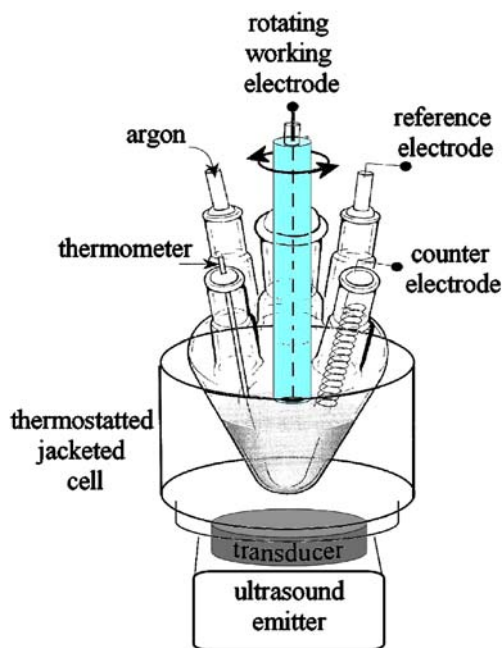


**Fig. 1** Schematic drawing of the thermostatted electrochemical cell for rotating disc voltammetry experiments in the presence of 500 kHz ultrasound

## Simulation of voltammetric current responses

For quantitative data analysis, cathodic limiting currents obtained at various electrode rotation rates and reagent concentrations were employed. The Digisim software package allows rotating disc voltammograms to be simulated based on the appropriate temperature,  $T=353$  K, the viscosity,  $\eta=0.0035$  cP, the diffusion coefficient (for the redox mediator 1,8-DHAQ,  $D=0.84\times 10^{-9}$  m<sup>2</sup> s<sup>-1</sup>), the concentrations, and further chemical parameters. For the mechanism a simple two-electron transfer followed by a chemical reaction step (vide infra) was chosen assuming that the colloid particles are small enough to be approximately represented by a homogeneous concentration parameter. The additional effects of colloidal particles on the mass transport at electrode surfaces described in the literature, for example, for CaCO<sub>3</sub> particles [18], is concentration dependent. Test experiments with indigo solutions and inert redox couples revealed no significant effect under conditions employed here, and therefore, these effects are not further considered.

## Results and discussion

Voltammetric characterisation of the reduction of solid indigo immobilized at the surface of a graphite electrode and immersed in aqueous buffer solution

It has been shown previously that solid indigo immobilized at a graphite electrode can be studied directly by electrochemical methods [7]. The microcrystalline solid is embedded in the electrode surface, and both reversible reduction and oxidation processes are observed. At room temperature two pH-dependent processes were observed and attributed to the two-electron reduction of indigo to leuco-indigo and the two-electron oxidation of indigo. It is shown here that these two processes depend on the solution temperature. Figure 2 shows cyclic voltammograms (double cycle) obtained for the reduction of solid indigo immobilized at a 4.9-mm-diameter graphite electrode and immersed in phosphate buffer at pH 7 (Fig. 2a,b) and at pH 12 (Fig. 2c). The two redox processes, P1 and P2, have been proposed to be consistent with mechanisms given in Eq. 1 [7].

At pH 7 the increase in temperature from 298 to 353 K had no significant effect on the electrochemical behaviour of the solid indigo. For the reduction process P1 a second

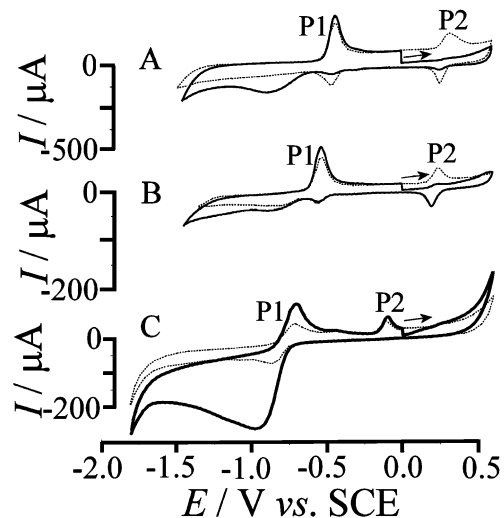
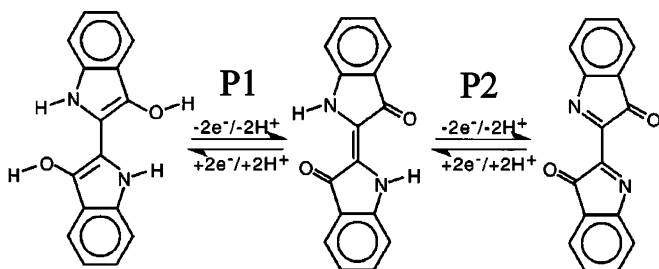


**Fig. 2** Cyclic voltammograms (scan rate, 0.1 V s<sup>-1</sup>) for the reduction and reoxidation of indigo microparticles immobilized at a 4.9-mm-diameter basal plane pyrolytic graphite electrode and immersed into 0.1 M phosphate buffer (pH 7) at 298 (a), and at 353 K (b), and pH 12 at 353 K (c)

voltammetric peak has been attributed to a process involving the Na<sup>+</sup> cation [7]. At pH 12 the reduction process P1 is associated with the deprotonation and solubilisation of indigo ( $pK_A\approx 12$ ), and the removal of indigo away from the electrode occurs. From the cathodic and anodic peak potentials the approximate reversible potential for the indigo/leuco-indigo systems at pH 12 and at 353 K can be estimated as  $-0.78$  V vs SCE, which provides a rough guide to predict the reactivity of indigo towards redox mediators. Next, the reduction process P1 was investigated in solution for colloidal indigo, and the effects of a redox mediator, 1,8-DHAQ, on the indigo reduction process are investigated.

Voltammetric characterisation of the 1,8-DHAQ mediator in the absence and presence of colloidal indigo

To investigate the redox properties of 1,8-DHAQ, first, rotating disc voltammetry experiments were conducted in the absence of indigo. Figure 3 shows a typical voltammetric response obtained at 80 °C (353 K) for a solution of 0.42 mM 1,8-DHAQ in 0.1 M phosphate buffer (pH 12). A well-defined reduction response was observed with a



(1)

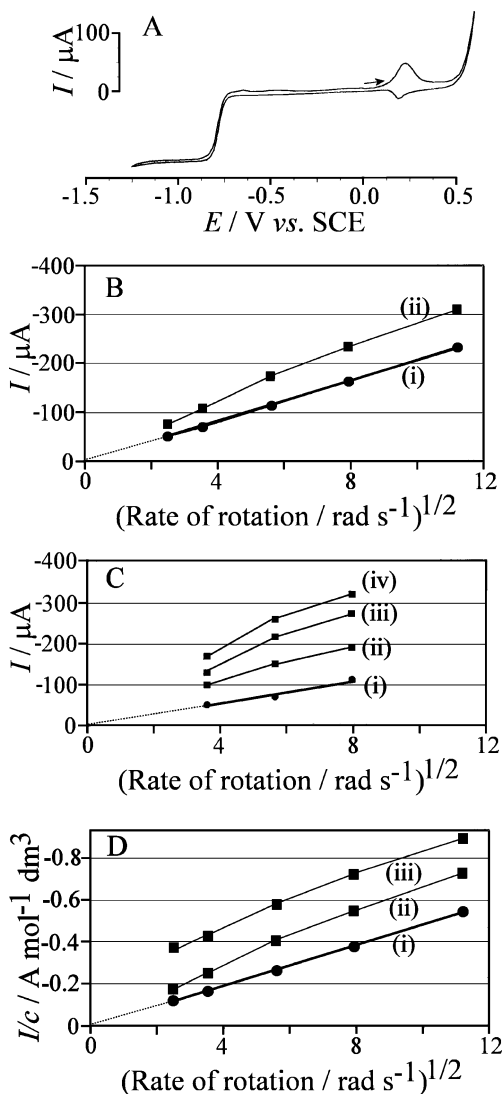


**Fig. 3** **a** Cyclic voltammogram (scan rate  $10 \text{ mV s}^{-1}$ ) for the reduction of  $0.42 \text{ mM}$  1,8-dihydroxyanthraquinone (1,8-DHAQ) in  $0.1 \text{ M}$  phosphate buffer pH 12 at a  $7\text{-mm}$ -diameter rotating gold disc electrode ( $5 \text{ Hz}$  rate of rotation) at  $353 \text{ K}$ . **b** Plot of the limiting currents for the reduction of 1,8-DHAQ vs the square root of the rate of rotation for a solution of  $0.42 \text{ mM}$  1,8-DHAQ without (i) and with (ii)  $2 \text{ mM}$  colloidal indigo. **c** Plot of the limiting currents for the reduction of 1,8-DHAQ vs the square root of the rate of rotation for a solution of  $0.3 \text{ mM}$  1,8-DHAQ without (i) and with  $2$  (ii),  $4$  (iii) and  $8 \text{ mM}$  (iv) colloidal indigo. **d** Plot of the limiting currents for the reduction of 1,8-DHAQ [curve (i) superimposed, curve (ii)  $0.42 \text{ mM}$  and curve (iii)  $0.042 \text{ mM}$  1,8-DHAQ] divided by the concentration versus the square root of the rate of rotation for solutions of 1,8-DHAQ (i) without and with (ii, iii)  $2 \text{ mM}$  colloidal indigo

reversible potential of  $-0.78 \text{ V}$  vs SCE. This reversible potential is very close to that observed for the reduction of indigo (vide supra). The Tomeš criterion [19], which is defined as the potential gap between the points where the current reaches three fourths and one fourth of the limiting current,  $E_{3/4} - E_{1/4} = 0.035 \text{ V} = 2.197 \times \frac{RT}{nF}$  ( $R$  is the gas constant,  $T$  the absolute temperature,  $F$  the Faraday constant, and  $n$  is the number of electrons transferred per molecule diffusing to the electrode surface), allows the

number of electrons transferred in this electrochemically reversible reduction process to be confirmed as  $n \approx 2$  consistent with the proposed mediator reaction in Scheme 1. The oxidation peak at  $0.2 \text{ V}$  vs SCE is consistent with a gold surface oxidation and not important in this study.

Next, the diffusion coefficient for 1,8-DHAQ at  $353 \text{ K}$  was determined. A plot of the limiting current observed during reduction vs the square root of the rate of rotation (see Fig. 3b) is linear, and therefore, the “Levich” equation [20] can be employed to determine the diffusion coefficient Eq. 2:

$$I_{\text{lim}} = 0.62 \times n F A c D^{2/3} \nu^{-1/6} \omega^{1/2}. \quad (2)$$

In this equation the mass-transport-controlled limiting current for the reduction,  $I_{\text{lim}}$ , is related to the number of electrons transferred per molecule diffusing to the electrode surface,  $n$ , the Faraday constant,  $F$ , the electrode area,  $A$ , the bulk concentration of 1,8-DHAQ,  $c$ , the diffusion coefficient,  $D$ , the viscosity at  $353 \text{ K}$ ,  $0.0035$ , and  $\omega$ , the rate of rotation. From data in Fig. 3b the diffusion coefficient in  $0.1 \text{ M}$  phosphate buffer (pH 12) and a temperature of  $80 \text{ }^\circ\text{C}$  ( $353 \text{ K}$ ) is  $D = (0.84 \pm 0.08) \times 10^{-9} \text{ m}^2 \text{ s}^{-1}$ . Consistent with Eq. 1 the current was observed to scale linearly with the concentration of the mediator 1,8-DHAQ. Alkaline solutions of 1,8-DHAQ were observed to undergo aging over several days, and therefore, fresh solutions have to be used for experiments.

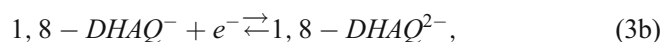
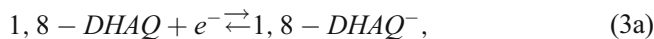
In the presence of only indigo in alkaline buffer solution, no significant electrochemical reduction current is observed in the absence of the redox mediator even at elevated temperatures of  $80 \text{ }^\circ\text{C}$  ( $353 \text{ K}$ ). This is consistent with a repulsive or inhibited interaction between colloidal indigo particles and the electrode surface. For other types of redox-active colloids such hydrous iron oxide direct interaction with suitable electrode surfaces and electron transfer have been demonstrated [21]. However, the current response observed for the redox mediator is substantially increased by the presence of indigo (see Fig. 3b–d), which is consistent with a mediated reduction of indigo particles. Figure 3c shows that increasing the concentration of indigo further increases the current for the mediated reduction process.

From the plots of the limiting current vs the square root of rotation rate, it can be seen that the current due to the indigo reduction is characteristically dependent on the rate of electrode rotation. To develop a better understanding of the overall process a simplistic mechanistic model based on a numerical simulation is developed next.

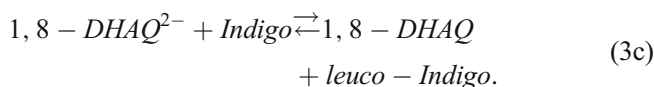
#### Analysis of rotating disc voltammetric data for the 1,8-DHAQ mediated indigo reduction

To achieve a more quantitative parameterization and understanding of the mediated indigo reduction process, a commercial software package for the simulation of voltammetric data, Digisim [15], is employed. Only the limiting

currents for the reduction process are considered and simulated. It is important to minimize the complexity of the model, and therefore, the following assumptions are introduced. The colloidal indigo is initially considered to be homogeneously distributed and treated as a molecular species. However, the diffusion coefficient for the indigo species is set to an extremely low limit (here,  $10^{-19} \text{ m}^2 \text{ s}^{-1}$ ) to reflect the low/insignificant mobility of colloidal particles. The mobility of the colloid particle is therefore entirely based on convective transport. The mechanism for the mediated indigo reduction is proposed to follow the following oversimplified (protonation equilibria are assumed to be fast and ignored) reaction sequence Eqs. 3a–c:



and



To further simplify the analysis, electron transfer in Eqs. 3a and 3b is assumed to be fast (reversible), the equilibrium constant for the process in Eq. 3c is fixed,  $K_{\text{eq}}=100$  (it is confirmed later that this parameter is not affecting the simulated limiting currents), and the forward rate constant for Eq. 3c,  $k_{\text{app}}$ , is introduced.

First, the current responses obtained in the absence of indigo are considered. Figure 3c shows the characteristic linear Levich behaviour of the current in relation to the square root of the rate of electrode rotation, and this behaviour is reproduced with the numerical simulation. The diffusion coefficient,  $D=0.8 \times 10^{-9} \text{ m}^2 \text{ s}^{-1}$  at 353 K, is employed for the 1,8-DHAQ mediator, and the simulated currents confirm the above analysis. Figure 4b (curve i) shows simulated limiting currents for the redox mediator 1,8-DHAQ in good agreement with experimental data (Fig. 3c).

Next, the effect of indigo is considered. Indigo particles are distributed within the solution phase, and transport of these particles into the diffusion or reaction layer is assumed to be entirely convection based (see Scheme 2). A characteristic increase in current was observed experimentally (see Fig. 3c) and is investigated here in two steps.

First, it is (erroneously) assumed that the reaction of 1,8-DHAQ with indigo is essentially mass-transport-limited, and the forwards rate constant for the chemical process in Eq. 3c is chosen extremely high ( $k_{\text{app}}=10^6 \text{ mol m}^{-3} \text{ s}^{-1}$ ) and thereby eliminated from the analysis. From the remaining simulation parameters, only the apparent concentration of indigo is taken to be free to allow the numerical current responses to be matched with experimental results. This approach apparently results in a reasonably good match between numerical data and the experimental data shown

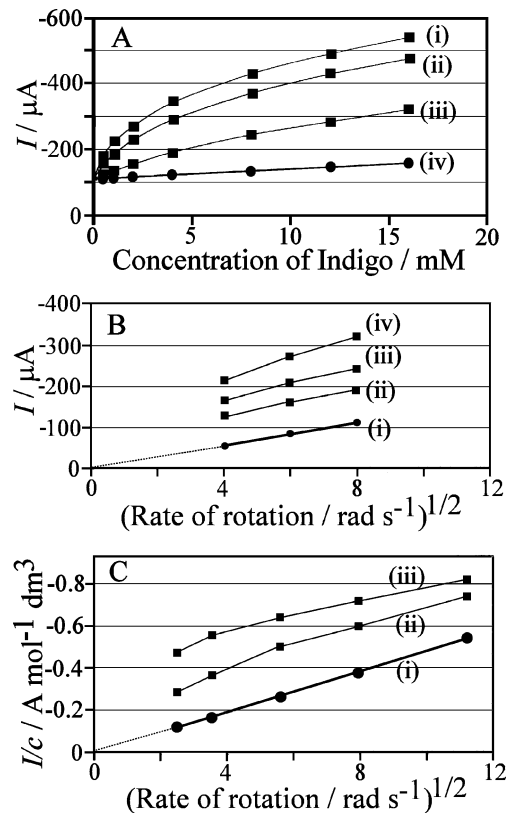
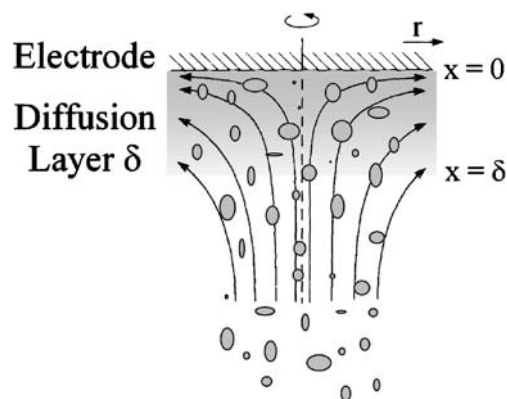


**Fig. 4** Simulated limiting currents for the reduction of 1,8-dihydroxyanthraquinone (1,8-DHAQ) in the absence and presence of indigo. **a** The effect of the indigo concentration on the limiting current for  $64 \text{ rad s}^{-1}$  rate of rotation,  $k=3 \times 10^4 \text{ mol m}^{-3} \text{ s}^{-1}$  (i),  $k=30 \text{ mol m}^{-3} \text{ s}^{-1}$  (ii),  $k=3 \text{ mol m}^{-3} \text{ s}^{-1}$  (iii),  $k=0.3 \text{ mol m}^{-3} \text{ s}^{-1}$  (iv) and 4 mM indigo. **b** The effect of indigo concentration [with 0 (i), 2 (ii), 4 (iii) and 8 mM (iv) indigo] on the limiting current for the reduction of 0.3 mM 1,8-DHAQ. **c** Normalised limiting currents for the reduction of 0.42 mM 1,8-DHAQ in the absence of indigo (i) and 0.42 (ii) and 0.042 mM (iii) 1,8-DHAQ in the presence of 2 mM indigo ( $k=3 \times 10^3 \text{ mol dm}^{-3} \text{ s}^{-1}$ )

in Fig. 3c using an apparent concentrations of 0.4, 0.8 and 1.6 mM indigo (the actual total concentrations were 2, 4 and 8 mM indigo based on weight of indigo per volume of solution, but initially, the apparent concentration was



**Scheme 2** Flow of particles towards a rotating disc electrode and the diffusion–reaction zone at the electrode surface/SCM

introduced to parameterize the lower observed limiting current). A good match of data was observed even for different indigo concentrations. However, when data for a low mediator concentration in Fig. 3d was simulated with the same set of parameters, a considerable mismatch was observed, and therefore, this approach was insufficient and abandoned (numerical data not shown). The use of at least two different mediator concentrations is important and has been used to eliminate the wrong simulation approach.

Second, a much better overall match of numerical and experimental data was observed when the forwards rate constant for the bimolecular reaction see Eq. 3c was allowed to control the limiting current. Figure 4a shows typical simulation results demonstrating the effect of the indigo concentration on the cathodic limiting current. In the absence of indigo or for very low chemical rate constants,  $k_{app}$ , a mediator-only current of  $-109 \mu\text{A}$  is determined. For a very high bimolecular rate constant,  $k=3 \times 10^4 \text{ mol m}^{-3} \text{ s}^{-1}$ , the expected diffusion-limited current is simulated, which is higher than the experimental current. Perhaps surprisingly, the diffusion-controlled current is not proportional to the concentration of indigo due to the second-order nature of the process. The higher the indigo concentration, the more mediator is used up and the more “compressed” the diffusion layer  $\delta$  becomes (see Scheme 2).

Next, to match experimental and simulation currents, the value of the apparent bimolecular rate constant is reduced. For an intermediate value of the apparent bimolecular rate constant,  $k_{app}=3 \text{ mol m}^{-3} \text{ s}^{-1}$ , the best agreement between simulation and experimental data is obtained. Figure 4b,c show simulation data in comparison to experimental data in Fig. 3c,d. A remaining trend towards higher simulation currents (compared to experimental currents) at lower rates of electrode rotation can be attributed to the depletion of smaller indigo particles, which leads to a change in the apparent rate constant towards smaller values (vide infra). However, overall, the match between experimental and simulation data is good even at different mediator concentrations.

Finally, the effect of the equilibrium constant for the process given in Eq. 3c on the kinetic analysis is considered. The reversible potential for both the reduction of indigo and the reduction of the mediator 1,8-DHAQ at 353 K is virtually identical, and therefore the (simplifying) choice of a very large equilibrium constant could be criticized. However, voltammetric data simulated for the process described by Eq. 3 are rather insensitive to the magnitude of this equilibrium constant, and even when set to unity, very similar currents are simulated. Therefore, the apparent bimolecular rate constant determined in this approach is reliable, and the physical meaning of the rate constant remains to be explored.

Interpretation of the bimolecular rate constant for the 1,8-DHAQ-mediated indigo reduction

It is interesting to consider the limits of the Digisim simulation approach and the physical meaning of the rate constant determined for the 1,8-DHAQ mediator. Indigo particles create their own diffusion field, and the rate of diffusion of the redox mediator towards the particle has to be considered. The apparent bimolecular rate constant determined experimentally has to be written as in Eq. 4:

$$\frac{d[\text{leuco} - \text{indigo}]}{dt} = k_{app} \times [\text{indigo}] \times [1, 5, 8, 9 - \text{THAQ}]. \quad (4)$$

The rate of formation of leuco-indigo is related to an apparent rate constant,  $k_{app}$ , the concentration of indigo and the concentration of the reduced form of the redox mediator. For the case of diffusion control this equation may also be written as in Eq. 5 [22]:

$$\frac{d[\text{leuco} - \text{indigo}]}{dt} = 4\pi r D \frac{N_A}{N_P} \times [\text{indigo}] \times [1, 5, 8, 9 - \text{THAQ}]. \quad (5)$$

In this equation the diffusion-controlled rate of formation of leuco-indigo is related to  $D$ , the diffusion coefficient for the redox mediator,  $N_A$ , Avogadro's number, and  $N_P$ , the number of indigo molecules per particle. Comparison of Eqs. 4 and 5 shows that the apparent rate constant for a diffusion-controlled process at the surface of a spherical particle of radius  $r$  is then given by Eq. 6.

$$k_{app} = 4\pi r D \frac{N_A}{N_P}. \quad (6)$$

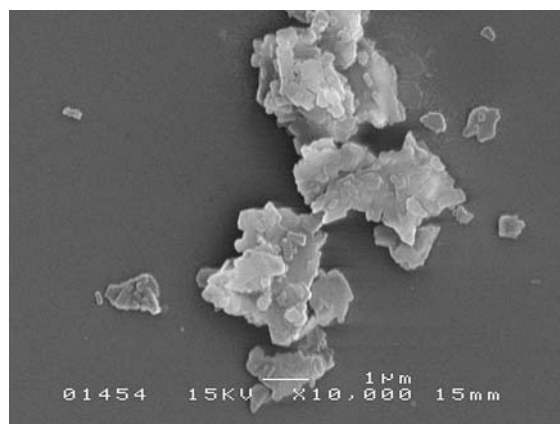


Fig. 5 SEM image of indigo microparticles

In this equation the parameters  $r$  (the particle radius) and  $N_p$  (the number of indigo molecules per particle) are related (by  $\frac{N_p}{N_A} \times \frac{M}{\rho} = 4\pi r^3$ , with the molecular mass  $M$  and the density  $\rho$ ), and with  $k_{app}$  known, they can be determined employing Eqs. 7 and 8:

$$r = \sqrt{\frac{DM}{k_{app}\rho}} \quad (7)$$

and

$$N_p = 4\pi N_A \sqrt{\frac{M}{\rho} \left(\frac{D}{k_{app}}\right)^3} \quad (8)$$

Using parameters determined in this study ( $k_{app}=3 \text{ mol m}^{-3} \text{ s}^{-1}$ ,  $D=0.84 \cdot 10^{-9} \text{ m}^2 \text{ s}^{-1}$ ,  $M=262 \text{ g mol}^{-1}$ , and  $\rho$  is assumed  $10^6 \text{ g m}^{-3}$ ), the approximate particle radius  $r=0.27 \text{ }\mu\text{m}$  and  $N_p=6 \times 10^8$  molecules are estimated. Comparison with a typical scanning electron micrograph (see Fig. 5) shows that these parameters are realistic, and that in solution, the plate-shaped indigo particles may indeed exhibit a radius between 0.1 and 0.5  $\mu\text{m}$ . However, the particles are clearly not spherical, which severely limits the viability of the above analysis.

A consistent mechanistic picture is obtained based on a diffusion-controlled reductive dissolution of colloidal indigo particles. The magnitude of the limiting current at a rotating disc electrode reflects the particle size of the colloid rather than a true bimolecular chemical rate constant. Treatments taking into account the distribution of particle sizes and particle shapes have appeared in the literature [23], but these parameters are beyond the scope of this study.

## Conclusions

The effectiveness of the redox mediator 1,8-DHAQ for the reduction of colloidal indigo has been investigated by rotating disc voltammetry. A detailed kinetic analysis suggests that essentially, diffusion-controlled reduction occurs, and that at a temperature of 353 K, 1,8-DHAQ is an excellent mediator system for the reduction of colloidal indigo. There are currently no comparable data for other redox mediator systems or for 1,8-DHAQ under other

reaction conditions. However, in the future, this experimentally simple approach based on rotating disc voltammetry and Digisim analysis will allow more detailed mechanistic information to be obtained and slow surface chemistry limited reactions to be identified.

**Acknowledgements** A.V. thanks MTT Agrifood Research Finland and the Finnish Cultural Foundation for financial support.

## References

1. Roessler A, Crettenand D (2004) *Dyes Pigm* 63:29
2. Compton RG, Perkin SJ, Gamblin DP, Davis J, Marken F, Padden AN, John P (2000) *New J Chem* 24:179
3. Roessler A, Jin X (2003) *Dyes Pigm* 59:223
4. McKenzie KJ, Marken F (2001) *Pure Appl Chem* 73:1885
5. Komorsky-Lovric S (2000) *J Electroanal Chem* 482(2000):222
6. Vickerstaff T (1954) *The physical chemistry of dyeing*. Oliver and Boyd, Edinburgh
7. Bond AM, Marken F, Hill E, Compton RG, Hügel H (1997) *J Chem Soc Perkin Trans II* 9:1735
8. Bechtold T, Turcanu A (2002) *J Electrochem Soc* 149:D7
9. Bechtold T, Turcanu A (2004) *J Appl Electrochem* 34:1221
10. Nicholson SK, John P (2005) *Appl Microbiol Biotechnol* 68:117
11. Bechtold T, Burtcher E, Turcanu A (1999) *J Electroanal Chem* 465:80
12. Roessler A, Crettenand D, Dossenbach O, Rys P (2003) *J Appl Electrochem* 33:901
13. Roessler A, Dossenbach O, Marte W, Rys P (2002) *J Appl Electrochem* 32:647
14. Roessler A (2003) *New electrochemical methods for the reduction of vat dyes*. Diss ETH Zürich No. 15120. Swiss Federal Institute of Technology, Zurich
15. Rudolph M, Reddy DP, Feldberg SW (1994) *Anal Chem* 66: A589
16. Scholz F, Schröder U, Gulaboski R (2005) *Electrochemistry of immobilized particles and droplets*. Springer, Berlin Heidelberg, New York
17. Komorsky-Lovric S, Mirceski V, Scholz F (1999) *Mikrochim Acta* 132:67
18. Compton RG, Brown CA (1993) *J Colloid Interface Sci* 158:243
19. Oldham KB, Myland JC (1994) *Fundamentals of electrochemical science*. Academic, London, p 291
20. Walsh F (1993) *A first course in electrochemical engineering*. The Electrochemical Consultancy, London, pp 131–132 (see for example)
21. McKenzie KJ, Marken F (2001) *Pure Appl Chem* 73:1885
22. Atkins PW (1998) *Physical Chemistry*. Oxford University Press, Oxford, p 827
23. Forryan CL, Klymenko OV, Brennan CM, Compton RG (2005) *J Phys Chem B Condens Mater Surf Interfaces Biophys* 109:8263